Imaging theory and resolution improvement of two-photon confocal microscopy

TANG Zhilie (唐志列)[1], YANG Chuping (杨初平)[2], PEI Hongjin (裴红津)[1], LIANG Ruisheng (梁瑞生)[1] & LIU Songhao (刘颂豪)[1]

1. Department of Physics, South China Normal University, Guangzhou 510631, China;
2. College of Sciences, South China Agricultural University, Guangzhou 510642, China
Correspondence should be addressed to Tang Zhilie (email: tangzhl@scnu.edu.cn)

Received February 10, 2002

Abstract The nonlinear effect of two-photon excitation on the imaging property of two-photon confocal microscopy has been analyzed by the two-photon fluorescence intensity transfer function derived in this paper. The two-photon fluorescence intensity transfer function in a confocal microscopy is given. Furthermore the three-dimensional point spread function (3D-PSF) and the three-dimensional optical transfer function (3D-OTF) of two-photon confocal microscopy are derived based on the nonlinear effect of two-photon excitation. The imaging property of two-photon confocal microscopy is discussed in detail based on 3D-OTF. Finally the spatial resolution limit of two-photon confocal microscopy is discussed according to the uncertainty principle.

Keywords: two-photon, confocal microscopy, resolution.

Two-photon confocal microscopy has attracted more and more attention recently, due to its supper-resolution imaging ability and unique 3D microfabrication ability. It has been widely used in life science[1—5], 3D-optical data storage[6—8], and lithographic microfabrication[9—11]. The imaging principles of confocal microscopy have been discussed extensively by many authors[12—15], but all of those theories failed to account for the nonlinear effect of two-photon excitation. Because the imaging process in two-photon confocal microscopy involves the nonlinear effect of two-photon excitation, the imaging property of two-photon confocal microscopy is very different from that of the conventional confocal microscopy. This nonlinear effect can improve the spatial resolution of confocal microscopy effectively. However, how this nonlinear effect affects the imaging property of confocal microscopy has not been discussed theoretically as far as we know. So these imaging theories cannot describe the imaging property of two-photon microscopy precisely[16]. According to the nonlinear characteristics of two-photon excitation, here we deduce the intensity transfer function of two-photon fluorescence in a confocal microscopy system. Furthermore, we deduce the three-dimensional point spread function (3D-PSF) and the three-dimensional optical transfer function (3D-OTF) of two-photon confocal microscopy using Fourier imaging theory and given the cut-off spatial-frequency based on 3D-OTF. Finally we discuss the spatial resolution limit of two-photon confocal microscopy according to the uncertainty principle.

1 Two-photon fluorescence point spread function in two-photon confocal microscopy

In order to derive 3D point spread function (3D-PSF) and 3D optical transfer function (3D-OTF) of two-photon confocal microscopy, we must first deduce two-photon fluorescence intensity transfer function of two-photon confocal microscopy. Fig. 1 shows the basic arrangement of a confocal microscopy. The light source function and the detector function are assumed to be a plane function and described by the following function respectively:

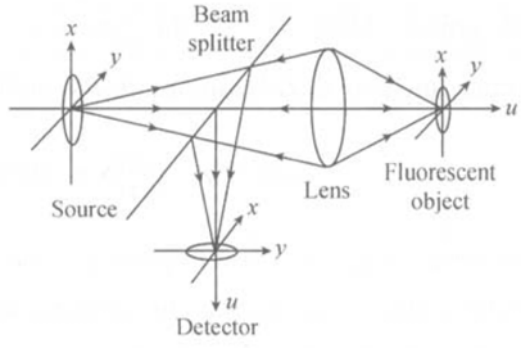

Fig. 1. Arrangement of confocal microscopy.

$$S(\boldsymbol{\upsilon}_s)=S(\upsilon_{sx},\upsilon_{sy};u_s)=S_1(\upsilon_{sx},\upsilon_{sy})\delta(u_s),\quad S_1(\upsilon_{sx},\upsilon_{sy})=\begin{cases}1, \upsilon_{sx}^2+\upsilon_{sy}^2\leqslant R_s^2,\\ 0,\ \text{others},\end{cases} \tag{1}$$

$$D(\boldsymbol{\upsilon}_d)=D(\upsilon_{dx},\upsilon_{dy};u_d)=D_1(\upsilon_{dx},\upsilon_{dy})\delta(u_d),\quad D_1(\upsilon_{sx},\upsilon_{sy})=\begin{cases}1, \upsilon_{dx}^2+\upsilon_{dy}^2\leqslant R_d^2,\\ 0,\ \text{others},\end{cases} \tag{2}$$

where R_s and R_d are the radii of the source and the detector, respectively (in terms of optical coordinate). Optical coordinate vectors on the source and detector plane are $\boldsymbol{\upsilon}_s(\upsilon_{sx},\upsilon_{sy};u_s)$ and $\boldsymbol{\upsilon}_d(\upsilon_{dx},\upsilon_{dy};u_d)$ respectively with

$$\begin{aligned}&\upsilon_{sx}=\frac{2\pi}{\lambda}x_s\sin\alpha,\upsilon_{sy}=\frac{2\pi}{\lambda}y_s\sin\alpha;u_s=\frac{2\pi}{\lambda}z_s\sin^2\alpha,\\ &\upsilon_{dx}=\frac{2\pi}{\lambda}x_d\sin\alpha,\upsilon_{dy}=\frac{2\pi}{\lambda}y_d\sin\alpha;u_d=\frac{2\pi}{\lambda}z_d\sin^2\alpha,\end{aligned} \tag{3}$$

where $\sin\alpha$ is the numerical aperture of the objective lens; (x_s, y_s, z_s) and (x_d, y_d, z_d) are Descartes coordinate of the source plane and the detector plane; $\boldsymbol{\upsilon}(\upsilon_x,\upsilon_y;u)$ is the optical coordinate vector of object plane.

The imaging process of two-photon confocal microscopy can be divided into two stages: one is that the point source S is focused on the object O by objective lens L, and the other is that two-photon fluorescence emitted from the object is focused on the detector by objective lens L and beam splitter BS. According to imaging theory[17], the imaging process from light source to the object plane is a coherent imaging process. So the complex amplitude distribution on the object plane is

$$U(\boldsymbol{\upsilon})=\iiint_{-\infty}^{\infty}S(\boldsymbol{\upsilon}_s)h(\boldsymbol{\upsilon}-\boldsymbol{\upsilon}_s)d\boldsymbol{\upsilon}_s \tag{4}$$

where $h(\boldsymbol{\upsilon}-\boldsymbol{\upsilon}_s)$ is the three-dimensional point spread function of the objective lens. Because

two-photon fluorescence intensity is proportional to the square of the incident light intensity or the biquadratic of amplitude. Let $O(\boldsymbol{\upsilon}_{\mathrm{p}}-\boldsymbol{\upsilon})$ represent the two-photon fluorescence spatial distribrtion function, which is determined by fluorescence efficiency and concentration of observed object. Here $\boldsymbol{\upsilon}_{\mathrm{p}}$ is the position vector of the scanned point. The two-photon fluorescence intensity distribution produced on the object plane can be expressed as

$$I_1(\boldsymbol{\upsilon}_{\mathrm{p}}-\boldsymbol{\upsilon})=\left|\iiint_{-\infty} S(\boldsymbol{\upsilon}_{\mathrm{s}})h(\boldsymbol{\upsilon}-\boldsymbol{\upsilon}_{\mathrm{s}})d\boldsymbol{\upsilon}_{\mathrm{s}}\right|^4 \cdot O(\boldsymbol{\upsilon}_{\mathrm{p}}-\boldsymbol{\upsilon}). \tag{5}$$

The second stage of the two-photon fluorescence imaging process from the object plane to the detector plane is an incoherent imaging process, so the two-photon fluorescence intensity distribution on the detector plane can be expressed as

$$I_2(\boldsymbol{\upsilon}_{\mathrm{d}},\boldsymbol{\upsilon}_{\mathrm{p}})=\iiint_{-\infty}\left\{\left|\iiint_{-\infty} S(\boldsymbol{\upsilon}_{\mathrm{s}})h(\boldsymbol{\upsilon}-\boldsymbol{\upsilon}_{\mathrm{s}})d\boldsymbol{\upsilon}_{\mathrm{s}}\right|^4 \cdot O(\boldsymbol{\upsilon}_{\mathrm{p}}-\boldsymbol{\upsilon})\right\}|h(\boldsymbol{\upsilon}_{\mathrm{d}}-\boldsymbol{\upsilon})|^2\, d\boldsymbol{\upsilon}. \tag{6}$$

Considering that the detector has a definite aperture $D(\boldsymbol{\upsilon}_{\mathrm{d}})$, the two-photon fluorescence intensity transfer function of the optical system shown in fig. 1 can be expressed as

$$\begin{aligned} I_3(\boldsymbol{\upsilon}_{\mathrm{p}}) &= \iiint_{-\infty}\left\{\iiint_{-\infty}\left\{\left|\iiint_{-\infty} S(\boldsymbol{\upsilon}_{\mathrm{s}})h(\boldsymbol{\upsilon}-\boldsymbol{\upsilon}_{\mathrm{s}})d\boldsymbol{\upsilon}_{\mathrm{s}}\right|^4 \cdot O(\boldsymbol{\upsilon}_{\mathrm{p}}-\boldsymbol{\upsilon})\right\}|h(\boldsymbol{\upsilon}_{\mathrm{d}}-\boldsymbol{\upsilon})|^2\, d\boldsymbol{\upsilon} \cdot D(\boldsymbol{\upsilon}_{\mathrm{d}})\right\}d\boldsymbol{\upsilon}_{\mathrm{d}} \\ &= \iiint_{-\infty}\left\{\left|\iiint_{-\infty} S(\boldsymbol{\upsilon}_{\mathrm{s}})h(\boldsymbol{\upsilon}-\boldsymbol{\upsilon}_{\mathrm{s}})d\boldsymbol{\upsilon}_{\mathrm{s}}\right|^4 \cdot \iiint_{-\infty}|h(\boldsymbol{\upsilon}-\boldsymbol{\upsilon}_{\mathrm{d}})|^2 D(\boldsymbol{\upsilon}_{\mathrm{d}})d\boldsymbol{\upsilon}_{\mathrm{d}}\right\}O(\boldsymbol{\upsilon}_{\mathrm{p}}-\boldsymbol{\upsilon})d\boldsymbol{\upsilon} \\ &= \{|S(\boldsymbol{\upsilon})\otimes_3 h(\boldsymbol{\upsilon})|^4 \cdot [|h(\boldsymbol{\upsilon})|^2 \otimes_3 D(\boldsymbol{\upsilon})]\}\otimes_3 O(\boldsymbol{\upsilon}_{\mathrm{p}}). \end{aligned} \tag{7}$$

According to the imaging theory, the image intensity equals the convolution of the light intensity of the object and the point spread function of the system; therefore, the three-dimensional point spread function of the imaging system shown in fig. 1 is

$$F(\boldsymbol{\upsilon})=\{[|S(\boldsymbol{\upsilon})\otimes_3 h(\boldsymbol{\upsilon})|^2 \cdot |S(\boldsymbol{\upsilon})\otimes_3 h(\boldsymbol{\upsilon})|^2] \cdot [|h(\boldsymbol{\upsilon})|^2 \otimes_3 D(\boldsymbol{\upsilon})]\}. \tag{8}$$

2 The sharpening process of two-photon fluorescence image

For confocal microscopy imaging system with point source and point detector, $S(\boldsymbol{\upsilon}_s)=\delta(\boldsymbol{\upsilon}_s), D(\boldsymbol{\upsilon}_d)=\delta(\boldsymbol{\upsilon}_d)$, the three-dimensional point spread function of the two-photon fluorescence confocal microscopy can be derived from eq. (8)

$$F_{\mathrm{con}}^{\mathrm{Two}}(\boldsymbol{\upsilon})=|h(\boldsymbol{\upsilon})|^6=\left|\iint_{-\infty} P(\xi,\eta)\exp\left[-\frac{ju}{2}(\xi^2+\eta^2)\right]\exp[-j(\upsilon_x\xi+\upsilon_y\eta)]d\xi d\eta\right|^6, \tag{9}$$

where $P(\xi,\eta)$ is the pupil function of the optical system, $\xi=\frac{x}{a},\eta=\frac{y}{a}$ are normalized Descartes

Coordinate, and *a* is the radius of the pupil.

To compare the 3D PSF of two-photon fluorescence confocal microscopy with that of single-photon fluorescence confocal microscopy and conventional fluorescence microscopy, we derived the 3D PSF of single-photon fluorescence confocal microscopy from eq. (9). It is well known that single-photon fluorescence is proportional to the intensity rather than the square of intensity of the incident light. The 3D point spread function of single-photon fluorescence confocal microscopy can also be derived from eq. (9) as

$$F_{\mathrm{con}}^{\mathrm{Single}}(\boldsymbol{\upsilon}) = |h(\boldsymbol{\upsilon})|^4 = \left| \iint_{-\infty} P(\xi,\eta) \exp\left[-\frac{ju}{2}(\xi^2+\eta^2) \right] \exp[-j(\upsilon_x \xi + \upsilon_y \eta)] d\xi d\eta \right|^4 . \tag{10}$$

For the conventional fluorescence microscopy, the 3D point spread function is

$$F_{\mathrm{flu}}^{\mathrm{Singl}}(\boldsymbol{\upsilon}) = |h(\boldsymbol{\upsilon})|^2 = \left| \iint_{-\infty} P(\xi,\eta) \exp\left[-\frac{ju}{2}(\xi^2+\eta^2) \right] \exp[-j(\upsilon_x \xi + \upsilon_y \eta)] d\xi d\eta \right|^2 . \tag{11}$$

Eqs. (9)—(11) shows that the 3D PSF of two-photon fluorescence confocal microscopy is much different from that of the single-photon fluorescence confocal microscopy and conventional fluorescence microscopy. In order to understand more clearly the imaging property of two-photon confocal microscopy, we discuss the lateral PSF and axial PSF below.

2.1 The lateral PSF of two-photon confocal microscopy

Let the axial coordinate $u = 0$ in eq. (9), the two-dimensional point spread function (2D PSF) on the focus plane of the objective lens can be written as

$$F_{con}^{Two}(\upsilon_x, \upsilon_y) = \left[\frac{2J_1(\sqrt{\upsilon_x^2+\upsilon_y^2})}{\sqrt{\upsilon_x^2+\upsilon_y^2}} \right]^4 \cdot \left[\frac{2J_1(\sqrt{\upsilon_x^2+\upsilon_y^2})}{\sqrt{\upsilon_x^2+\upsilon_y^2}} \right]^2 . \tag{12}$$

Obviously, if one writes out single-photon fluorescence confocal microscopy and conventional fluorescence microscopy by letting the axial coordinate $u = 0$ in (10) and (11) as

$$F_{\mathrm{con}}^{\mathrm{Single}}(\upsilon_x, \upsilon_y) = \left[\frac{2J_1(\sqrt{\upsilon_x^2+\upsilon_y^2})}{\sqrt{\upsilon_x^2+\upsilon_y^2}} \right]^4 , \tag{13}$$

$$F_{\mathrm{flu}}^{\mathrm{Single}}(\upsilon_x, \upsilon_y) = \left[\frac{2J_1(\sqrt{\upsilon_x^2+\upsilon_y^2})}{\sqrt{\upsilon_x^2+\upsilon_y^2}} \right]^2 , \tag{14}$$

the 2D PSF of two-photon fluorescence confocal microscopy explicitly equals the product of single-photon fluorescence confocal microscopy and conventional fluorescence microscopy. Their numerical plots are displayed in fig. 2(a).

From fig. 2 (a), we can draw the conclusions as follows:

(ⅰ) The 2D PSF of two-photon confocal microscopy is sharper than that of single-photon

confocal microscopy due to the nonlinear effect of two-photon transition rather than the confocal optical system, because the optical system employed in the two cases is identical. That means the nonlinear effect of two-photon transition can cause the fluorescence image to sharpen and realize supper resolution imaging.

(ii) It is the sharpest of 2D PSF in two-photon confocal microscopy among all kinds of fluorescence microscopy because there are two sharpening processes in two-photon confocal microscopy: one is due to the nonlinear effect of two-photon transition; the other is due to the confocal system. So two-photon confocal microscopy has the highest lateral resolution in all kinds of fluorescence microscopy.

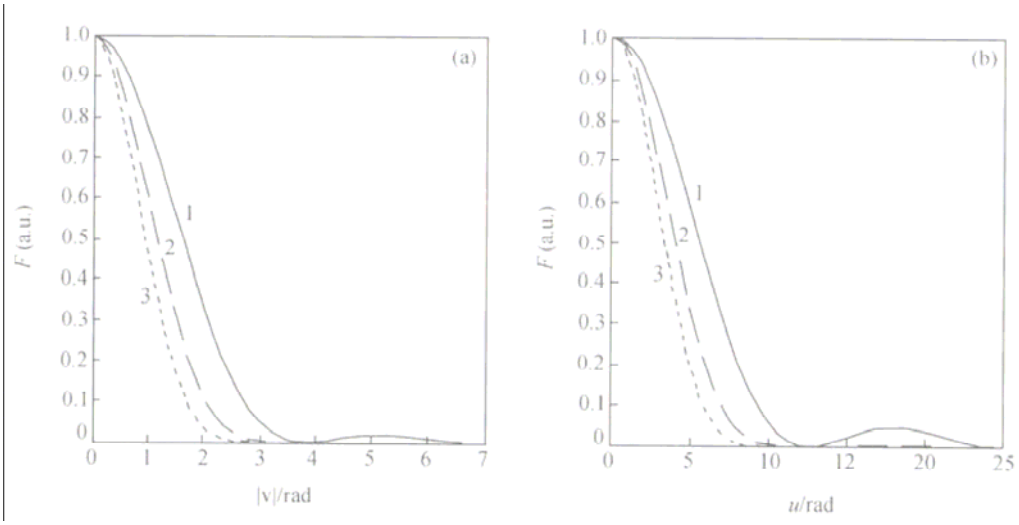

Fig. 2. The lateral fluorescence point spread function (a) and the axial fluorescence point spread function in different kinds of microscopy. 1, Single-photon fluorescence microscopy; 2, single-photon confocal microscopy; 3, two-photon confocal microscopy.

2.2 The axial PSF of two-photon confocal microscopy

Letting the lateral coordinate $\upsilon_x = 0,\ \upsilon_y = 0$ in eq. (9), one can obtain the axial PSF of two-photon confocal microscopy

$$F_{\text{con}}^{\text{Two}}(0,0;u) = \left[\frac{\sin(u/4)}{u/4}\right]^4 \bullet \left[\frac{\sin(u/4)}{u/4}\right]^2. \tag{15}$$

For single-photon fluorescence confocal microscopy and conventional fluorescence microscopy, the axial PSF by letting the lateral coordinate $\upsilon_x = 0,\ \upsilon_y = 0$ in eqs. (10) and (11) is

$$F_{\text{con}}^{\text{Single}}(0,0;u) = \left[\frac{\sin(u/4)}{u/4}\right]^4. \tag{16}$$

$$F_{\text{flu}}^{\text{Single}}(0,0;u) = \left[\frac{\sin(u/4)}{u/4}\right]^2. \tag{17}$$

From (15)—(17), we can see that the axial PSF of two-photon confocal microscopy is equal to the

product of the axial PSF of single-photon fluorescence confocal microscopy and that of the conventional microscopy, Their numerical plots are displayed in fig. 2(b).

From fig. 2(b), we can reach the same conclusion as the lateral one. In conclusion, two-photon confocal microscopy has the highest lateral resolution and axial resolution among all kinds of fluorescence microscopy, because there are two sharpness processes in the two-photon confocal microscopy: one is due to the nonlinear effect of two-photon transition, and the other is due to the confocal system.

3 Frequency domain analysis of two-photon confocal microscopy

In order to understand more clearly the nonlinear effect of two-photon transition on the imaging property of two-photon confocal microscopy, let us examine the imaging process in frequency domain. According to the imaging theory, the imaging property of an optical system can be described completely by the optical transfer function (OTF).

3D OTF of two-photon confocal microscopy together with the 3D OTF for a single-photon confocal microscopy and the conventional fluorescence microscopy have to be derived. We introduce the normalized spatial frequency for simplicity:

$$\nu_x = \frac{\lambda}{\sin\alpha} f_x; \qquad \nu_y = \frac{\lambda}{\sin\alpha} f_y; \qquad \mu = \frac{\lambda}{\sin^2\alpha} f_z. \tag{18}$$

Here f_x, f_y, f_z are the spatial frequencies.By taking the Fourier transform of eq. (12), we can obtain the 3D OTF of conventional microscopy as follows:

$$H_{flu}(\nu;\mu) = \begin{cases} \dfrac{1}{\nu}[1-(\dfrac{|\mu|}{\nu}+\dfrac{\nu}{2})^2]^{1/2} & , |\nu| \leqslant 2, \quad |\mu| \leqslant \nu - \dfrac{\nu^2}{2} \leqslant \dfrac{1}{2}. \\ 0 & , \qquad \text{others} \end{cases} \tag{19}$$

Eq. (19) shows that the cut-off lateral frequency and axial frequency are $|\nu| \leqslant 2, |\mu| \leqslant 1/2$ respectively. By taking the Fourier transform of (10) and using (19), we can obtain the 3D OTF of single-photon confocal microscopy as follows:

$$\begin{aligned} H_{\text{flu}}^{\text{Singl}}(\nu_x,\nu_y;\mu) &= \Im\left\{|h(\upsilon)|^4\right\} = \Im\left\{|h(\upsilon)|^2\right\} \otimes_3 \Im\left\{|h(\upsilon)|^2\right\} \\ &= \iiint_{-\infty} \frac{1}{[(x+\frac{\nu_x}{2})^2+(y+\frac{\nu_y}{2})^2]^{1/2}[(x-\frac{\nu_x}{2})^2+(y-\frac{\nu_y}{2})^2]^{1/2}} \\ &\times \left\{1-\left[\frac{|z+\frac{\mu}{2}|}{[(x+\frac{\nu_x}{2})^2+(y+\frac{\nu_y}{2})^2]^{1/2}} + \frac{[(x+\frac{\nu_x}{2})^2+(y+\frac{\nu_y}{2})^2]^{1/2}}{2}\right]^2\right\}^{1/2} \\ &\times \left\{1-\left[\frac{|z-\frac{\mu}{2}|}{[(x-\frac{\nu_x}{2})^2+(y-\frac{\nu_y}{2})^2]^{1/2}} + \frac{[(x-\frac{\nu_x}{2})^2+(y-\frac{\nu_y}{2})^2]^{1/2}}{2}\right]^2\right\}^{1/2} dxdydz \end{aligned} \tag{20}$$

From eq. (20), the following inequality must be satisfied :

$$|z+\frac{\mu}{2}| \leqslant \left[\left(x+\frac{\nu_x}{2}\right)^2+\left(y+\frac{\nu_y}{2}\right)^2\right]^{1/2} - \frac{\left[\left(x+\frac{\nu_x}{2}\right)^2+\left(y+\frac{\nu_y}{2}\right)^2\right]}{2}$$

$$= -\frac{1}{2}\left\{\left[\left(x+\frac{\nu_x}{2}\right)^2+\left(y+\frac{\nu_y}{2}\right)^2\right]^{1/2}-1\right\}^2+\frac{1}{2}\leqslant\frac{1}{2}. \tag{21}$$

$$|z-\frac{\mu}{2}| \leqslant \left[\left(x-\frac{\nu_x}{2}\right)^2+\left(y-\frac{\nu_y}{2}\right)^2\right]^{1/2} - \frac{\left[\left(x-\frac{\nu_x}{2}\right)^2+\left(y-\frac{\nu_y}{2}\right)^2\right]}{2}$$

$$= -\frac{1}{2}\left\{\left[\left(x-\frac{\nu_x}{2}\right)^2+\left(y-\frac{\nu_y}{2}\right)^2\right]^{1/2}-1\right\}^2+\frac{1}{2}\leqslant\frac{1}{2}. \tag{22}$$

From (21) and (22), we obtain

$$|\nu| \leqslant 4, |\mu| \leqslant 1. \tag{23}$$

Inequality (23) shows that the cut-off lateral freuency and axial frequency are 4 and 1,respectively, twice those of a conventional fluorescence microscopy.

After taking the Fourier transform of (9) and using (19), the 3D OTF of two-photon confocal microscopy can be expressed as

$$H_{\text{con}}^{\text{Two}}(\nu_x,\nu_y;\mu) = \Im\left\{|h(\upsilon)|^4 \cdot |h(\upsilon)|^2\right\} = \Im\left\{|h(\upsilon)|^4\right\} \otimes_3 \Im\left\{|h(\upsilon)|^2\right\}$$

$$= \iiint_{-\infty}^{\infty}\iiint_{-\infty}^{\infty} \frac{1}{\left\{\left[\left(m-\frac{\nu_x}{2}\right)\right]^2+\left[\left(n-\frac{\nu_y}{2}\right)\right]^2\right\}^{1/2}}$$

$$\cdot \frac{1}{\left[\left(x+\frac{\left(m+\frac{\nu_x}{2}\right)}{2}\right)^2+\left(y+\frac{\left(n+\frac{\nu_y}{2}\right)}{2}\right)^2\right]^{1/2}} \quad \frac{1}{\left[\left(x-\frac{\left(m+\frac{\nu_x}{2}\right)}{2}\right)^2+\left(y-\frac{\left(n+\frac{\nu_y}{2}\right)}{2}\right)^2\right]^{1/2}}$$

$$\cdot\left\{1-\left[\frac{\left|z+\frac{\left(l+\frac{\mu}{2}\right)}{2}\right|}{\left[\left(x+\frac{\left(m+\frac{\nu_x}{2}\right)}{2}\right)^2+\left(y+\frac{\left(n+\frac{\nu_y}{2}\right)}{2}\right)^2\right]^{1/2}}+\frac{\left[\left(x+\frac{\left(m+\frac{\nu_x}{2}\right)}{2}\right)^2+\left(y+\frac{\left(n+\frac{\nu_y}{2}\right)}{2}\right)^2\right]^{1/2}}{2}\right]^2\right\}^{1/2}$$

$$\cdot\left\{1-\left[\frac{\left|z-\frac{\left(l+\frac{\mu}{2}\right)}{2}\right|}{[(x-\frac{(m+\frac{\nu_x}{2})}{2})^2+(y-\frac{(n+\frac{\nu_y}{2})}{2})^2]^{1/2}}+\frac{\left[\left(x-\frac{\left(m+\frac{\nu_x}{2}\right)}{2}\right)^2+\left(y-\frac{\left(n+\frac{\nu_y}{2}\right)}{2}\right)^2\right]^{1/2}}{2}\right]^2\right\}^{1/2}$$

$$\cdot\left\{1-\left[\frac{\left|l-\frac{\mu}{2}\right|}{\left\{\left[\left(m-\frac{\nu_x}{2}\right)\right]^2+\left[\left(n-\frac{\nu_y}{2}\right)\right]^2\right\}^{1/2}}+\frac{\left\{\left[\left(m-\frac{\nu_x}{2}\right)\right]^2+\left[\left(n-\frac{\nu_y}{2}\right)\right]\right\}^{2^{1/2}}}{2}\right]^2\right\}^{1/2}$$

$$\cdot dxdydzdmdndl. \tag{24}$$

which leads to the following inequalities:

$$\left|l-\frac{\mu}{2}\right|\leqslant\frac{1}{2}. \tag{25}$$

$$|z+\frac{l+\frac{\mu}{2}}{2}|\quad\left[\left(x+\frac{m+\frac{\nu_x}{2}}{2}\right)^2+\left(y+\frac{n+\frac{\nu_y}{2}}{2}\right)^2\right]^{1/2}\quad-\frac{\left[\left(x+\frac{m+\frac{\nu_x}{2}}{2}\right)^2+\left(y+\frac{n+\frac{\nu_y}{2}}{2}\right)^2\right]}{2}$$

$$= -\frac{1}{2}\left\{\left[\left(x+\frac{m+\frac{\nu_x}{2}}{2}\right)^2+\left(y+\frac{n+\frac{\nu_y}{2}}{2}\right)^2\right]^{1/2}-1\right\}^2+\frac{1}{2}\quad\frac{1}{2}. \tag{26}$$

$$\left|z-\frac{l+\frac{\mu}{2}}{2}\right|\left[\left(x-\frac{m+\frac{\nu_x}{2}}{2}\right)^2+\left(y-\frac{n+\frac{\nu_y}{2}}{2}\right)^2\right]^{1/2}-\frac{\left[\left(x-\frac{m+\frac{\nu_x}{2}}{2}\right)^2+\left(y-\frac{n+\frac{\nu_y}{2}}{2}\right)^2\right]}{2}$$

$$= -\frac{1}{2}\left\{\left[\left(x-\frac{m+\frac{\nu_x}{2}}{2}\right)^2+\left(y-\frac{n+\frac{\nu_y}{2}}{2}\right)^2\right]^{1/2}-1\right\}^2+\frac{1}{2}\leqslant\frac{1}{2}. \tag{27}$$

From inequalities (25)—(27), we obtain

$$|\nu|\leqslant 6, |\mu|\leqslant\frac{3}{2}. \tag{28}$$

Inequality (28) shows that the cut-off lateral frequency and axial frequency are 6 and 3/2, respectively, which are about the sum of those of single-photon fluorescence confocal microscopy and conventional fluorescence microscopy. This is resonable because the 3D OTF of two-photon confocal microscopy is the convolution of those of single-photon fluorescence confocal microscopy and conventional fluorescence microscopy. According to the convolution theorem[18], the width of convolution is about the sum of that of the two convolutional functions.

From secs 3 and 4, we know that the nonlinear effect of two-photon transition can sharpen the 3D PSF and widen the spatial frequency bandwidth of OTF. And this property can greatly improve the spatial resolution of two-photon confocal microscopy.

4 The resolution limit of two-photon confocal microscopy

In order to understand the supper resolution imaging ability of two-photon confocal microscopy, we derive its resolution limit in terms of uncertainty principle. According to the uncertainty principle, when a photon from a definite point passes throuth an optical imaging system (called measuring system), its uncertainty of transverse coordinate x on the imaging plane is determined by $\Delta P_x \cdot \Delta x \approx h$. The momentum of a photon is $P_x = \hbar k_x = f_x h$, here, k_x is the wave vector of x axis, and f_x is the spatial frequency in x direction. Hence the uncertainty of coordenate x of the photon passing through the optical imaging system is determined by

$$\Delta f_x \cdot x \geqslant 1, \tag{29}$$

where Δf_x is the transmitted bandwidth of spatial frequency in *x* direction. For the coordinate *z* of optical axis, we have

$$\Delta f_z \cdot \Delta z \geqslant 1, \tag{30}$$

where Δf_z is the transmitted bandwidth of axial spatial frequency. Substituting formula (18) into (29) and (30) , we have

$$\Delta \nu_x \cdot \Delta x \geqslant \frac{\lambda}{\sin\alpha}, \qquad \Delta\mu \cdot \Delta z \geqslant \frac{\lambda}{\sin^2\alpha}. \tag{31}$$

The resolution limit of any kind of microscopy can be derived as follows:

(i) For conventional fluorescence microscopy, its transmitted bandwidth of lateral frequency and axial frequency are $\Delta\nu_x$=2, $\Delta\mu$=1/2, respectively according to formula (19); therefore, the uncertainties of lateral coordinate and axial cordinate are respectively

$$\Delta x_{\text{flu}} \geqslant \frac{\lambda}{2\sin\alpha} \approx \frac{\lambda}{2a} d_{\text{i}}, \tag{32}$$

$$\Delta z_{\text{flu}} \geqslant \frac{2\lambda}{\sin^2\alpha}, \tag{33}$$

where *a* is the radius of pupil; d_{i} is the distance of image. It is obvious that Δx_{flu} is the radius of Airy disc, and Δz_{flu} is the focal depth of the objective lens. Therefore when a lot of photons pass through the optical imaging system, they will image an Ariy disc on the imaging plane and form a focal depth along the *z* axis on the imaging plane.

(ii) For two-photon confocal microscopy, its transmitted bandwidth of lateral frequency and axial frequency are $\Delta\nu_x = 6, \Delta\mu = 3/2,$ respectively. So the uncertainties of lateral coordinate and axial coordinate are

$$\Delta x_{\text{con}}^{\text{Two}} \geqslant \frac{\lambda}{6\sin\alpha}, \tag{34}$$

$$\Delta z_{\text{con}}^{\text{Two}} \geqslant \frac{2\lambda}{3\sin^2\alpha}. \tag{35}$$

From eqs. (34) and (35), it can be shown that the lateral resolution limit is $\lambda/(6 \cdot \sin\alpha)$, and axial resolution limit is $2\lambda/3\sin^2\alpha$.

5 Conclusion

The nonlinear effect of two-phonton transition has an important effect on the imaging property of two-photon confocal microscopy, which can sharpen the 3D PSF and widen the transmitted bandwidth of spatial frequency. Because of this nonlinear effect, the point spread function of two-photon fluorescence confocal microscopy is identical to the product of those of

the confocal microscopy and conventional microscopy, and the OTF of two-photon fluorescence confocal microscopy is equal to the convolution of that of confocal microscopy and the conventional microscopy. Therefore, the point image of two-photon fluorescence in a confocal microscopy system experiences two processes of sharpening: one is due to the nonlinear effect of two-photon transition, and the other is due to the confocal system. The spatial resolution of two-photon confocal microscopy is therefore much higher than that of confocal microscopy and conventional fluorescence microscopy.

References

1. Denk, W., Strickler, J. H., Webb, W. W., Two-photon laser scanning fluorescence microscopy, Science, 1990, 248(6): 73—76.
2. Kano, H., Kawata, S., Two-photon-excited fluorescence enhanced by a surface plasmon, Opt. Lett., 1996, 21(22): 1848—1850.
3. Bewersdorf, J., Pick, R., Hell, S. W., Multifocal multiphoton microscopy, Opt. Lett., 1998, 23(9): 655—657.
4. Hell, S. W., Booth, M., Wilms, S., Two-photon near- and far-field fluorescence microscopy with continuous-wave excitation, Opt. Lett., 1998, 23(15): 1238—1240.
5. Sanchez, E. J., Novotny, L., Xie, X. S., Near-Field fluorescence microscopy based on two-photon excitation with metal tips, Phys. Rev. Lett., 1999, 82(20): 4014—4017.
6. Parthenopoulos, D. A., Rentzepis, P. M., Three-dimensional optical storage memory, Science, 1989, 245, 843—845.
7. Strickler, J. H., Webb, W. W., Three-dimensional optical data storage in refractive media by two-photon point excitation, Opt. Lett., 1991, 16(22): 1780—1782.
8. Xia, A. D., Wada, S., Tashiro, H., Optical data storage in C_{60} doped polystyrene film by photo-oxidation, Appl. Phys. Lett., 1998, 73(10): 1323—1325.
9. Cumpstem, B. H., Ananthavel, S. P., Barlow, S. et al., Two-photon polymerization initiators for three-dimensional optical data storage and microfabrication, Nature, 1999, 398(4): 51—54.
10. Maruo, S., Nakamuro, O., Kawata, S., Three-dimensional microfabrication with two-photon-absorbed photopolymerization, Opt. Lett., 1997, 22(2): 132—134.
11. Sun, H. B., Matsuo, S., Misawa, H., Three-dimensional photonic crystal structures achieved with two-photon- absorption photopolymerization of resin, Appl. Phys. Lett., 1999, 74(6): 786—788.
12. Sheppard, C. J. R., Mao, X. Q., Three-dimensional imaging in a microscope, J. Opt. Soc. Am., 1989, 6(9): 1260—1269.
13. Min Gu, Sheppard, C. J. R., Analysis of confocal microscopy under ultrashort light-pulse illumination: comment, J. Opt. Soc. Am., A, 1994, 11(10): 2742—2743.
14. Kemepe, M., Rudolph W., Analysis of confocal microscopy under ultrashort light-pulse illumination, J. Opt. Soc. Am. A., 1993, 10(2): 240—245.
15. Min Gu, Sheppard, C. J. R., Three-dimensional image formation in confocal microscopy under ultra-short-laser-pulse illumination, J. Mod. Opt., 1995, 42(4): 747—762.
16. Tang Zhi-lie, Liang Rui-sheng, Chang Hong-shen, The theory of two-photon confocal microscopy, Acta Physica Sinica, 2000, 49(6): 1076—1080.
17. Goodman, J. W., Introduction to Fourier Optics, New York: McGraw-Hill,1968.
18. Gaskill, J. D., Linear System, Fourier Transform and Optics, New York: John Wiley & Sons, Inc., 1978.